Publications of the Astronomical Society of Australia (2018), **35**, e034, 10 pages
doi:10.1017/pasa.2018.38

CAMBRIDGE UNIVERSITY PRESS

Research Paper

Photometric and spectroscopic variability of the Be star 48 Lib: The relation between photometric variations and rotation

D. Ozuyar[1,2], S. Caliskan[1], I. R. Stevens[2] and A. Elmasli[1]

[1]Ankara University, Faculty of Science, Department of Astronomy and Space Sciences, 06100, Tandogan, Ankara, Turkey and [2]School of Physics and Astronomy, University of Birmingham, Edgbaston, Birmingham B15 2TT, UK

Abstract

The purpose of this paper is to determine the origin of the photometric variations of 48 Lib using the data from the *STEREO* and to investigate their relations with the disk structure. The photometric data comprise a period of five years from 2007 to 2011. The spectroscopic data covering the same time interval are provided from the *BeSS* database. The Hα lines are examined by measuring their equivalent widths and line intensities. Hα variations are then compared with those displayed by the photometric data. From the photometry, high-precision results (10^{-5} c d^{-1} in frequency and 10^{-4} mag in amplitude) are obtained. It is detected that the star has shown 24 frequencies, mainly clustered around the peaks at 2.48896(1) and 5.08150(2) c d^{-1}. The analysis reveals that the photometric frequencies are not due to pulsation, but caused by the rotation, and that the remaining frequencies arise from transient activities on or just above the photosphere. Also, it is shown that the spectroscopic data exhibit a significant Hα variability, and that the Hα line variation depends on the variation of frequency and amplitude, something which has been often proposed in the literature but has never before been demonstrated observationally. This proves that the disk structure and photometric variations are related.

Keywords: methods: data analysis – stars: emission line, Be – stars: individual: 48 Lib – stars: rotation

(Received 26 April 2018; Revised 18 September 2018; Accepted 25 September 2018)

1. Introduction: Be Stars

The general definition of a Be star is given by Collins (1987) as *a non-supergiant B star whose spectrum has, or at some time had, one or more Balmer lines in emission*. However, this definition is clearly quite broad and contains all B-type stars with emission lines due to circumstellar material with densities greater than about 10^{-13} g cm^{-3}. Based on this definition, stars that have a luminosity class of V–III with emission lines should be classified as a Be star regardless of their physical differences. Yet, there are some distinctions that separate objects commonly termed *classical Be stars* from those emission line objects of other provenance such as Herbig stars or mass transferring systems (Rivinius, Carciofi, & Martayan 2013).

Classical Be stars are Population I type, main sequence (MS), or slightly evolved B stars with a spectral range of late-O to early-A (Neiner et al. 2009) and a luminosity class of V–III (Zorec & Briot 1997). Their surface temperatures are between 10 000 and 30 000 K. Unlike normal B stars, unusual Balmer emission lines, singly ionised metals, and neutral He are seen in their spectra. Approximately 20% of B stars are classified as Be stars (Percy 2007), and most of these are of spectral types B1 and B2 (Porter & Rivinius 2003).

Despite sharing the same region with β Cephei and slowly pulsating B (SPB) stars on the H–R diagram, Be stars are quite different in a number of ways, such as their rapid rotation velocities. The average rotational velocity of these extremely fast rotators is roughly 88% of their critical break-up velocity (Frémat et al. 2005). It is also reported that the mean equatorial velocity for early-type Be stars is quite lower than the estimated critical rotational velocity ($v/v_{cr} \approx 0.6$). v/v_{cr} ratio increases to ≈ 0.8 for late Be stars, which means only the late Be stars may be rotating near critical rotational velocities (Balona 2013a).

Be stars show periodic or quasi-periodic line profile variations closely resembling the variations expected from non-radial pulsation (NRPs) (Rivinius, Baade, & Štefl 2003; Gutiérrez-Soto et al. 2007). The observed variability is believed to arise from both high-order g-modes and low-order p-/g-modes, depending on the temperature and depth of the iron opacity bump within Be stars. It is thought that pulsations probably play an important role in mass ejection and are the additional mechanism required for disk formation since they are excited even in late-type Be stars, as in β CMi (Saio et al. 2007).

In order to confirm such a suggestion, several spectroscopic and photometric investigations have been conducted. For instance, the spectroscopic study of Rivinius et al. (1998) indicates that the beating of pulsating modes can be the cause of the mass-loss episodes in μ Cen. Goss et al. (2011) report that α Eri shows correlations between the pulsation amplitude and disk activity. Also, *CoRoT* 102719279 exhibits a strong pulsational amplitude increase, coincident with a general fading, believed to be caused by the newly ejected matter (Gutiérrez-Soto et al. 2010). For HD 49 330, the observed strength of the short-period p-modes decreases while the those of longer transient periods arise during outbursts (Huat et al. 2009).

Author for correspondence: D. Ozuyar, Email: dozuyar@ankara.edu.tr

Cite this article: Ozuyar D, Caliskan S, Stevens IR and Elmasli A. (2018) Photometric and spectroscopic variability of the Be star 48 Lib: The relation between photometric variations and rotation. *Publications of the Astronomical Society of Australia* **35**, e034, 1–10. https://doi.org/10.1017/pasa.2018.38

© Astronomical Society of Australia 2018; published by Cambridge University Press.

Downloaded from https://www.cambridge.org/core. Ankara Universitesi, on 12 Dec 2021 at 00:02:46, subject to the Cambridge Core terms of use, available at https://www.cambridge.org/core/terms. https://doi.org/10.1017/pasa.2018.38

The photometric data obtained from the space telescopes such as the *MOST* or *CoRoT* show that several Be stars have multi-periodic light characteristics. As previously mentioned, these variations are attributed to non-radial g-mode pulsations of high radial order. However, it is not noticed that the multi-periodicity seen in their light curves is not steady. Also, these stars have a typical broad peak and its harmonic in their periodograms. This observed peak is close to the rotational frequency and its first harmonic due to the low frequencies of high-order g-modes in the co-rotating frame (Balona 2013a).

Independent from the duration of the observation, the broad structure of the peaks remains unchanged. Among these peaks, a periodic signal is seen as a quite narrow peak. If the photometric data are examined by dividing them into various subsets, it is seen that the frequencies obtained for each set are different from each other. Therefore, it can be deduced that the variations in the light of these stars are stochastic (Balona 2013a). Moreover, it is known that variations in amplitude and in structure of the broad peaks, which cause the changes in light curve, are another characteristic of Be stars. Since these photometric changes are connected to the line profile variations, it can be inferred from this connection that the line profile variations are just an indication of this stochastic process and not related to pulsation (Balona 2013a).

Even though popular models suggest that pulsations are the trigger of the mass ejections, for pulsation to set off an ejection, the horizontal component of pulsational velocity should be considered, such that it is added to the rotational velocity so as to exceed the circular orbital velocity at the equator. However, the pulsational velocity is quite low (only some tens of km s^{-1}) and for this reason, the star must be rotating very close to the critical velocity. At extreme rotational speeds, gravitational darkening comes into prominence and causes smaller line broadening which shows a much smaller value of $v \sin i$ than it should be (Townsend, Owocki, & Howarth 2004).

Since late type Be stars have larger $v \sin i$ values compared to the early Be stars and the rotational velocities of Be stars are commonly interpreted to be close to critical values, the corrections of the gravity darkening for late B stars are quite small. Contrarily, since the $v \sin i$ values of early Be stars are low (0.4–0.6 and up to v_{cr}, Cranmer 2005), the gravity darkening correction for these stars is quite large. Despite these facts, the theoretical calculations of the NRP hypothesis for gravitational darkening give opposite result, and it cannot explain why early Be stars need a large gravitational darkening correction (Townsend et al. 2004). The idea behind the NRP hypothesis regarding to Be stars is based on the fact that only stars with outer convective layers can have spots and flares. However, several observational studies carried out since 2009 have suggested that inhomogeneous regions can be produced on O-, A-, and B-type stars (Degroote et al. 2009; Balona 2014a, 2016). Additionally, Cantiello & Braithwaite (2011) theoretically show that magnetic fields at the stellar surface of radiative stars can produce bright spots.

While NRP hypothesis is unable to explain most of the obvious characteristics of Be stars, their major properties can be easily explained with a simple concept of magnetic acceleration of a flare-like event on a B-type star. There is also no need to consider that all Be stars rotate near their critical rotational velocity. This idea is supported with the statistical analysis conducted by Balona (1995), who shows that the fundamental photometric periods of Be stars derived from their light curves agree with rotational velocity measurements (rotational periods). Balona (2013a) also suggests that periodic variations seen in both line profiles and light curves of Be stars are simply a result of a localised mass-loss process, which produces gas concentrations (cloud) that co-rotate with the star. Accordingly, it is argued that the gas is localised and rotates with the star at the densest phase of the gas after the mass ejection. This causes to be a light variation having a period equal to the rotational period. At the later stages, the gas dissipates, phase coherence disappears, and the stochastic variations occur (Balona 2013a).

Table 1. Archival frequency values for 48 Lib

Frequency (c d^{-1})	Type	Reference
8.70	Radial velocity	(1)
1.52, 2.49	Photometric	(2)
2.49	Photometric	(3)
1.25, 1.36, 3.10	Spectroscopic	(4)
3.70, 7.50, 10.60		
0.227, 0.551	Spectroscopic	(5)

(1) Ringuelet-Kaswalder (1963); (2) McDavid (1988); (3) Cuypers, Balona, & Marang (1989); (4) Floquet et al. (1996); (5) Bossi et al. (1994).

In the light of the information given above, this paper is organised as follows to have a better understanding of the effects of pulsation and rotation on photometric variations seen in 48 Lib. Accordingly, Section 2 introduces 48 Lib and briefly mentions its archival studies. While Section 3 describes the *STEREO* satellite and explains the pipeline used to obtain the photometric light curves, Section 4 presents the photometric results as well as the rotational modulation of 48 Lib. Section 5 and Section 6 give the details of Hα line profile analysis and the results, respectively. Finally, Section 7 summarises the overall study and discusses the results.

2. Literature Review of 48 Lib

48 Lib (FX Lib; HD 142 983; HIP 78 207; HR 5 941) ($V = 4.94$ mag) is a well-studied Be shell star. Although it is classified as a B8Ia/Iab-type supergiant (Catanzaro 2013; Lafrenière et al. 2014; Peña-Guerrero & Leitherer 2013), many researchers consider the star to be an early-type sub-giant, giant, or MS object (B3III to V) (Hanuschik & Vrancken 1996; Draper et al. 2014; Štefl et al. 2012; Touhami et al. 2013; Silaj et al. 2016). Similar to most Be stars, it is a rapid rotator with a projected rotational velocity ($v \sin i$) of around 400 km s^{-1} (Štefl et al. 2012; Touhami et al. 2013) and a critical rotational velocity of ∼500 km s^{-1} (Frémat et al. 2005; Silaj et al. 2016). This rapid rotation is the main reason of the problems experienced for spectral classification.

Using various observational techniques, several periodicities of the star have been reported in the literature (see Table 1). McDavid (1988) and Cuypers et al. (1989) found a photometric period of ∼2.49 cycle per day (c d^{-1}). Cuypers et al. (1989) also characterised the photometric variation of the light curves as being rather asymmetrical, with a sharp rise and a gradual decline.

Hanuschik & Vrancken (1996) observed a double-peaked Hα profile, with asymmetric V and R components (with $V/R < 1$). Okazaki (1997) suggested that V/R ratios showed four individual periodic cycles with the length of 7.5, 10, 12, and 13.5 yr between 1950 and 1994. Although Štefl et al. (2012) stated that there was no V/R variation between 1995 and 1998, they detected

Downloaded from https://www.cambridge.org/core. Ankara Universitesi, on 12 Dec 2021 at 00:02:46, subject to the Cambridge Core terms of use, available at https://www.cambridge.org/core/terms.
https://doi.org/10.1017/pasa.2018.38

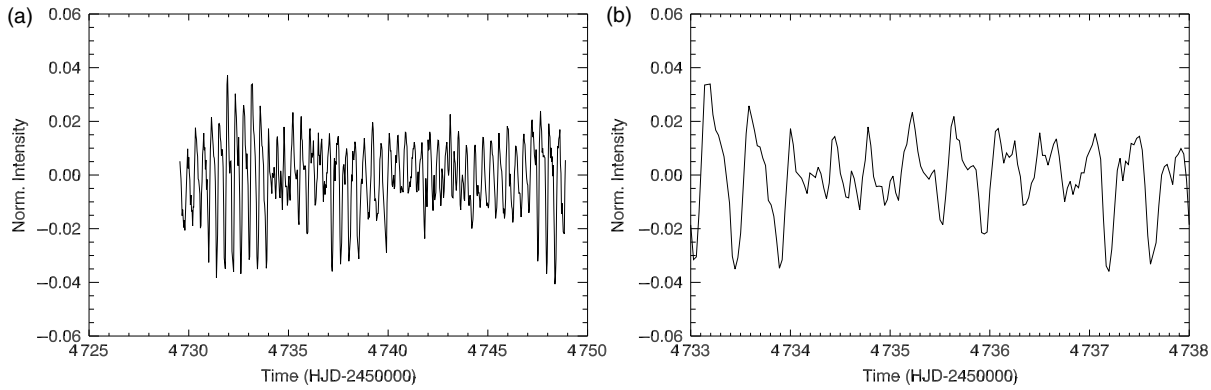


Figure 1. (a) The STEREO 2008 light curve of 48 Lib after the refinement procedure. The *x*-axis represents the observation duration whereas the *y*-axis shows normalised flux count ($(F(t)/\bar{F}) - 1$). (b) The 5-d data period that covers between HJD 2 454 733 and HJD 2 454 738.

a longer cycle period (∼17 yr) after 1998. Under the assumption of a constant orbital angular momentum (rotational parameter, $j = 1$) and Keplerian rotation ($j = 1/2$), Gunasekera, Adassuriya, & Medagangoda (2008) calculated the radii of the disk to be 2.64 and 6.98 $R_\star$, respectively. Also, Štefl et al. (2012) suggested a dense inner disk quite close to or contacting to the star. Accordingly, they obtained the outer radius as 15 $R_\star$ for the H continuum disk and 30−50 $R_\star$ for the diameter of Br_γ emitting region, assuming that the star was a B3V-type MS object with a stellar radius of 3.56 $R_\odot$. This result, which agreed with the findings of Pott et al. (2010), revealed that 48 Lib had one of the largest angular diameters among Be stars.

Haubois et al. (2012) studied dynamical evolution of viscous disks around Be stars. According to the study, the colour, magnitude, and the long-term *V/R* variation of 48 Lib were correlated. To this respect, they suggested that the photometric variability was not related to variability of the mass injection rate but to the one-armed density wave in the disk. In other words, the photometric variation was connected with *V/R* cycle.

Recently, Silaj et al. (2016) reproduced the photometric, polarimetric, and spectroscopic observables of 48 Lib with a viscous decretion disk model and tested the global oscillation scenario. They calculated the disk perturbation with a two-dimensional global oscillation code and obtained a very good, self-consistent fit to the time-averaged properties of the disk. The calculated perturbation had a period of ∼12 yr. Thus, they improved the fit to the photometric data and reproduced some features of the observed spectroscopic data. Consequently, they determined the spectral type of the star as B3V. The inclination of the star-disk system was found to be 85° by examining the polarisation levels. The mass and the polar radius of the star were also given as 6.07 $M_\odot$ and 3.12 $R_\odot$, respectively. Assuming that the linear velocity at the stellar equator, $v_{eq} = 400$ km s^{-1} ($\sin i \approx 1$), they found that $v_{eq}/v_{cr} \approx 0.80$ for the models with the mass 6.07 $M_\odot$.

3. Photometric Observations

The *STEREO* mission is the third of the NASA *Solar Terrestrial Probes* programme. It consists of two identical spacecraft in heliocentric orbits at a radii of around 1 au. The *STEREO-A* orbits ahead of the Earth, while the *STEREO-B* lags behind it: they are not fixed with respect to the planet, but rather drift from each other by 44° per year.

The main task of *STEREO* is to monitor photospheric activities of the Sun as well as the development and propagation of coronal mass ejections. The satellites carry several instrument packages for fulfilling these missions, one of which is the *Sun Earth Connection Coronal and Heliospheric Investigation* (*SECCHI*) including the *Heliospheric Imagers (HI)*. Photometric data are produced by these imagers which point near to the solar disk and monitor brightness of background stars around the ecliptic (V = 12 mag or brighter).

The *HI-1* instruments have a 20° by 20° field of view (FOV) and consequently can observe stars for ∼20 d each year, with a 40-min cadence, while the *HI-2* instruments have a 70° by 70° FOV and a 2-h cadence. The spectral response of the *HI* instruments is very broad (450–950 nm). For details of the *HI* instruments refer to Eyles et al. (2009) and Bewsher et al. (2010).

Only the data from the *HI-1A* instrument are used for this study. A more detailed description of the basic light curves can be found in Sangaralingam & Stevens (2011) and Whittaker, Stevens, & Sangaralingam (2013). Seasonal data comprise an observation interval of ∼20 d. The cadence of the data is a photometry point every 40 min, meaning that there are a maximum of 720 data points in each data portion. However, the usable number of data points is often less than this, due to some satellite-related problems or tracking errors in the data analysis. Such an observation set gives an opportunity to perform analysis in a wide frequency range, with the Nyquist frequency of around 18 c d^{-1}. The main goal of this study is to identify as many oscillation frequencies as possible in the photometric data and to catch potential correlations with spectroscopic observations. For this reason, the light curves obtained are needed to be decontaminated from internal and external effects caused by the circumstances mentioned by Sangaralingam & Stevens (2011). Therefore, long-term variations are removed from the light curves by using a third-order polynomial fitting, and observation points greater than 3σ are clipped.

Thus, we derive a maximum of 682 data points from the *HI-1A* in an observation season (in 2011), and a total of 3 098 observation points (covering ∼97 d) in 5 yr. Although the data taken in 2007, 2008, and 2011 are largely unaffected, the data in the 2009 and 2010 seasons are more affected by instrumental problems. Despite this, the light curves are suitable for the analyses. A sample of cleaned light curves is shown in Figure 1, and detailed information about the seasonal and combined light curves is given in Table 2.

Downloaded from https://www.cambridge.org/core. Ankara Universitesi, on 12 Dec 2021 at 00:02:46, subject to the Cambridge Core terms of use, available at https://www.cambridge.org/core/terms.
https://doi.org/10.1017/pasa.2018.38

Table 2. Details of the seasonal and combined (Comb.) observations of 48 Lib

Time (yr)	Mid-Obs. Time (HJD)	Data Pnt. (raw no.)	Data Pnt. (cleaned no.)
2007	2 454 395	611	598
2008	2 454 739	680	668
2009	2 455 084	662	579
2010	2 455 428	680	571
2011	2 455 773	685	682
Comb.		3 318	3 098

Observation years, mid-times of each observation, and the numbers of raw and cleaned data points are given in the columns. Due to some satellite-related problems such as pointing discontinuity or tracking error, the numbers of seasonal raw data points are less than the maximum 720 data points.

All seasonal data and the combined time series are analysed with the Lomb–Scargle (LS) algorithm. During the analyses, the number of independent frequencies is calculated with $N_{\rm raw}/2$, where $N_{\rm raw}$ is the number of raw observation points, in order to derive reliable results, and false alarm probability is assumed to be 99% ($P_0 = 0.01$). Signals are sought in the frequency range of 0.03–10 c d^{-1}. The specific significance level is calculated with the help of the equation:

$$z = -\sigma_0^2 \ \ln\Big(1 - (1 - P(z)\Big)^{1/N_{\rm id}}. \qquad (1)$$

In this equation, $\sigma_0 = A_{\rm m}\sqrt{N}/2$; where $A_{\rm m}$ is the mean amplitude of the amplitude spectrum, $P(z)$ is the false alarm probability, and $N_{\rm id}$ is the number of independent frequency. Since the z significance level is in the unit of power, the corresponding amplitude is derived from $A_z = 2\sqrt{z/N}$ (Balona 2014b). Also, the noise profile of the periodogram is determined for every 0.5 c d^{-1} frequency interval, to use in the equation. The significance levels are presented with red dashed lines in the periodograms.

4. Photometric Results

In this investigation, we detect 24 frequencies above the significance threshold in the 5 yr of combined periodogram. The amplitude spectra consist of two dominant frequency groups at 2.48896(1) and 5.08150(2) c d^{-1}. As seen in Figure 2, the former is the main frequency ($A = 9.34$ mmag) and agrees with the findings of McDavid (1988) and Cuypers et al. (1989). The spacing between the frequencies in each group is calculated to be around 0.08 c d^{-1}. In addition, we find two lower frequencies at 0.10927(5) and 0.19915(4) c d^{-1}. Of these, the latter one is relatively close to the result given by Bossi et al. (1994).

The primary frequency generally appears at around 2.49 c d^{-1} during the 5-yr time interval (Figure 2). However, this frequency shows an unusual change in 2008 by decreasing to 2.35 c d^{-1}. Considering only those changes at around 2.49 c d^{-1}, we realise that it exhibits a beat-like variation in 2007, 2008, 2010, and 2011. We also observe an abnormal increase of about 0.01 c d^{-1} in 2009 for the same frequency. Analogous with this variability, the frequencies at around 2.17 and 4.95 c d^{-1} have the same beat-like change over 5 yr. Apart from these, we detect seven frequencies at around 2.20, 2.24, 2.32, 2.37, 2.42, 2.59, and 5.08 c d^{-1} in the seasonal periodograms. These frequencies are regularly identified in each amplitude spectrum and also observed in the 5-yr combined data set. The variations in 2.42

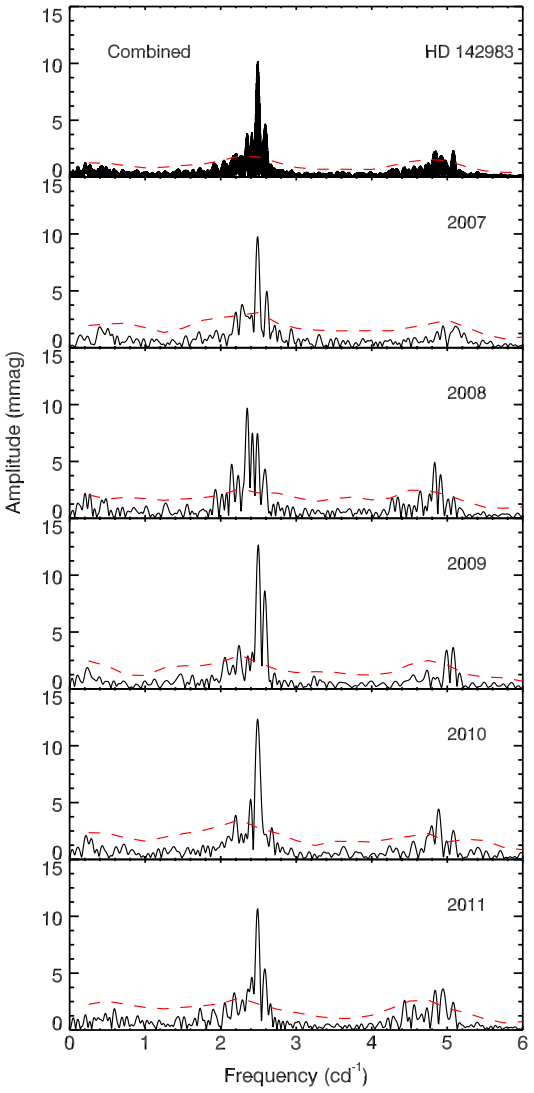


Figure 2. Five-year combined and seasonal amplitude spectra of 48 Lib. The variability is concentrated around two dominant frequency regions, at around 2.49 and 5.00 c d^{-1}. The red dashed lines show the noise levels calculated for every 0.5 c d^{-1} frequency interval.

and 2.59 c d^{-1} are quite similar, such that they both decrease and show an unusual drop in 2010. Also, the frequencies at 2.20 and 2.32 c d^{-1} demonstrate a decreasing change between 2007 and 2011. Besides, 2.24 c d^{-1} displays an increasing frequency profile.

The amplitudes of these frequencies are also variable. The most remarkable changes occur in the amplitudes of 2.49 c d^{-1} and the seasonal main frequencies. They show a sinusoidal variation with the minimum in 2008 and the maximum in 2010. In addition, the amplitude of 2.20 c d^{-1} has a decreasing change, whereas the amplitudes of 2.17, 2.32, 2.37, and 2.42 c d^{-1} exhibit a similar variation with an abnormal increase in 2008.

In addition, we also apply a sliding-window method to all individual data to check every possible frequency and amplitude variations as a function of time. The length of the window is set as 5 d, and it is shifted across the seasonal light curves with a time step of 1 d. In each step, we perform a Fourier analysis by using the LS technique and plot results against the time as in Figure 3.

Downloaded from https://www.cambridge.org/core. Ankara Universitesi, on 12 Dec 2021 at 00:02:46, subject to the Cambridge Core terms of use, available at https://www.cambridge.org/core/terms.
https://doi.org/10.1017/pasa.2018.38

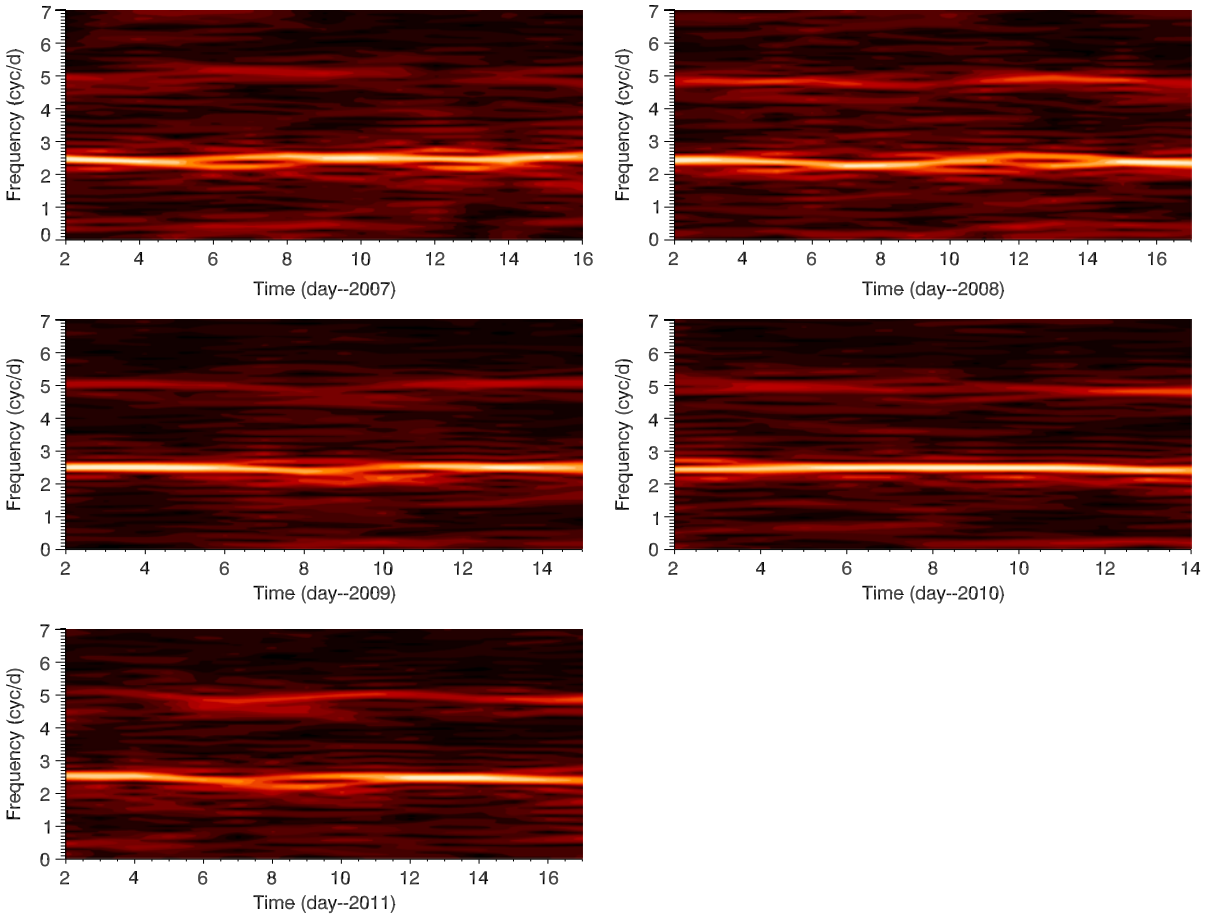


Figure 3. Sliding-window method applied to all individual data to check frequency and amplitude variations as a function of time. The length of the sliding window is 5 d and shifted across the seasonal light curves with the step of 1 d. The mid-points of 5-d sliding windows are used in the *x*-axis.

In the figure, the frequencies at around 2.49 and 5.00 c d^{-1} show up clearly and persistently. However, the rest of the frequencies seem to be more temporary and last in a few days. The variation at around 2.49 c d^{-1} is always the most dominant structure over the course of 5 yr. Although the frequency of this variation is constant, except in 2008 ($f_1 = 2.351$ c d^{-1}), it shows daily and seasonal amplitude changes. The frequency at around 5.00 c d^{-1} is also conspicuous. The most remarkable changes in its amplitude take place in 2008 and 2011. The interesting feature for this frequency is periodic modulations, particularly in 2011, with peak-to-peak period of around 10 d ($\sim$0.1 c d^{-1}). Additionally, as seen from Figure 3, both frequencies are split into two parts (e.g. between the observation days of 8 and 11 in 2011 for the frequency at 2.49 c d^{-1}) and the spacing between these splits is around 0.1 c d^{-1}. This value is quite consistent with the regular spacing seen between the frequencies in the amplitude spectrum.

4.1. Rotational modulation?

As seen in the frequency spectrum of 48 Lib, the star shows explicit multi-periodicities. However, the structural similarities and constancies of the dominant frequencies at 2.48896(1) and 5.08150(2) c d^{-1}, and the presence of transient frequencies presented in Figure 3 provide a critical evidence that these multi-periodicities are more likely a result of rotation rather than pulsation. Additionally, amplitudes of the frequencies seen in the periodograms display variations which may be a signature of non-uniformly distributed regions on the photosphere or circumstellar material. Such changes are suggested to be related to a change in the size of the spot regions or possible drift in latitude (Balona et al. 2011). Also, the frequencies at around 2.17, 2.49, and 4.95 c d^{-1} exhibit beat-like variations over 5 yr, as discussed in the previous section. This beating effect may also be considered to be originated by inhomogeneous regions in differential rotation (Balona 2016). Therefore, the features given as visible harmonic, variable amplitudes, and beating in the light curve make 48 Lib a good candidate that shows rotational modulation. For this reason, the existence of surface or circumstellar inhomogeneities should be considered for this star (Balona 2009).

Such a rotational modulation can be confirmed from the phased light curves of both 5 yr of combined and seasonal data given in Figures 4 and 5. The folded light curve of the combined data is produced by using the data obtained between 2007 and 2011 and using the main frequency given as 2.48896 c d^{-1}. The outliers greater than 3σ are removed from the data. As seen from the figure, the curve has a single sinusoid and clearly asymmetric shape, with major difference in the steepness of the ascending and descending branches: the rising branch is noticeably steeper than the descending one. This type of modulation is attempted to be explained for ξ Per by Ramiaramanantsoa et al. (2014). The authors find out the presence of a few co-rotating magnetic bright spots with the same period as the rotation period of the star. In the

Downloaded from https://www.cambridge.org/core. Ankara Universitesi, on 12 Dec 2021 at 00:02:46, subject to the Cambridge Core terms of use, available at https://www.cambridge.org/core/terms.
https://doi.org/10.1017/pasa.2018.38

Table 3. The parameters derived from the spot model

Inclination angle	85°
Limb darkening	0.4
Latitude of the spot	10°
Longitude of the spot	205°
Radius of the spot	24°
Relative brightness of the spot	0.6

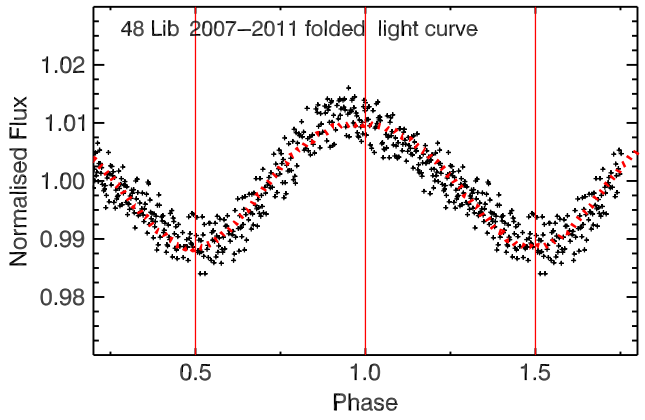


Figure 4. The folded light curve of the entire data set taken between 2007 and 2011. The curve has a single and smooth sinusoidal-like variation with an asymmetry, such that the rising branch is steeper than the descending one. The red curve represents the theoretical light variation produced by a spot model.

case of 48 Lib, it is not clear whether such a change can be caused by the presence of a large magnetic spot or multiple spots on the stellar surface.

In order to explain the cause of the asymmetric light modulation seen in the star, the only thing to do is to show how easy it is to obtain a reasonable fit using the simplest possible spot model. In such a model, whose math can be found in Dorren (1987), we assume that the inclination angle of the star is around 85° (Silaj et al. 2016) and the star has a single circular spot. By entering various spot parameters, we attempt to generate a theoretical light curve that best fits the real observational data. As a result of several trials, we obtain an acceptable fit which explains the curve with the minimum of free parameters. The fit is shown in Figure 4 with the red dashed line, and the related parameters are given in Table 3.

As seen from the figure, observational and theoretical data sets are quite compatible with each other ($\chi^2 = 0.0080$), which means that the variation seen in the light can be represented by a single-spotted rotation model in the simplest way. However, this by no means is a unique solution, and of course there is not only one solution. Also, the feature causing the light variation does not have to be a single spot. It is possible to make a really good fit by assuming many spots having different lifetimes, sizes, or positions on the star, but this is not very rational since a large number of free parameters have to be adjusted. On the other hand, it does not even have to be a spot. Most likely, it has nothing to do with a sunspot, but is merely some obscuration which is co-rotating with the star. It is actually not possible to know the real solution since there are not enough observations on colour, spectroscopic data, etc., which might constrain the solution.

5. Spectroscopic Observations

In order to investigate the relationship between the photometric and spectroscopic characteristics, spectroscopic observations in the BESS database[a] are used.

We examine a number of spectra of 48 Lib in BESS taken from several telescopes/instruments. For this analysis, we only consider optical spectra having a resolution of 6 000–17 000 and covering the Hα line. Heliocentric velocity corrections are applied to all spectra, and telluric lines occurred due to absorption within the atmosphere are removed by using a reference spectrum that creates a telluric template. Final data are shown in Figure 6.

For the EW measurements of the Hα lines, there are two uncertainties arising from the continuum normalisation and noise caused by telluric lines. The most significant one is related to the continuum normalisation. Therefore, we follow the process described by Jones, Tycner, & Smith (2011) and assume that the error of the normalisation is 3%. Then, we carry out the analysis with the SPLOT package of IRAF (noao–onedspec–splot) and measure the EW values.

In addition, the intensities of the components of the Hα line are evaluated. Since 48 Lib has a double-peaked line profile, the maximum intensities of V and R components are separately measured by subtracting each maximum intensity from the continuum line, and the V/R ratios are calculated from

$$V/R = \left[F(V) - F_c\right] / \left[F(R) - F_c\right], \quad (2)$$

where $F(V)$ and $F(R)$ are raw intensities of V and R components, F_c is the level of continuum line.

6. Spectroscopic Results

For a better understanding of spectroscopic effects, 20 spectra taken between 2007 and 2011 and a spectrum obtained in 1993 are examined. Only the results covering the period between 2007 and 2011 are presented in order to compare them with the photometric findings derived in the same time interval. The evolution of the emission components and the EW of the Hα profile are shown in Figure 6.

The spectra show a strong and narrow absorption line surrounded by violet (V) and red (R) emission components, indicating the existence of a circumstellar disk. There is also no indication of narrow optical absorption components in any of these spectra. As shown in the figure, the peak intensities vary in time. Although the V component is dominant until HJD 2 454 967, the intensity of R component starts to increase after HJD 2 455 037. Further, they remain almost symmetrical between these dates.

In order to measure the V/R ratio, we calculate peak heights above the zero flux level and present a powerful V/R variation that is likely caused by a one-armed density wave of the disk in Figure 7. Accordingly, we take the opportunity to observe the decreasing branch of a long-term disk variability, which is also presented in detail by Štefl et al. (2012). This decrement is probably about to reach its minimum phase.

In addition, we derive the EW values of the Hα profiles and find that these values have a decreasing variation (Figure 7). Also, this decreasing structure seems to contain quasi-periodic cycles with the period of around 2.16(14) yr and the amplitude of 0.76(12) Å.

[a] http://basebe.obspm.fr/basebe/.

Downloaded from https://www.cambridge.org/core. Ankara Universitesi, on 12 Dec 2021 at 00:02:46, subject to the Cambridge Core terms of use, available at https://www.cambridge.org/core/terms.
https://doi.org/10.1017/pasa.2018.38

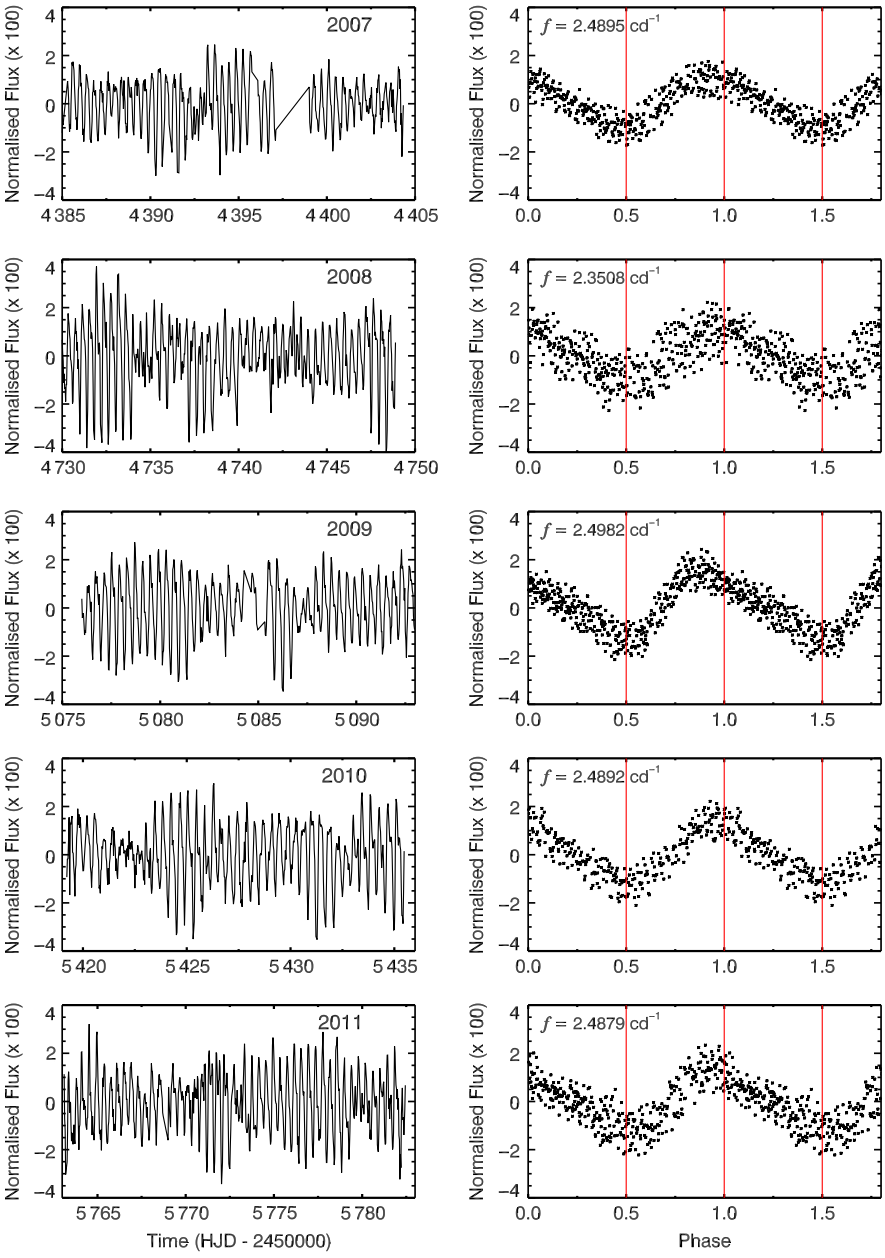


Figure 5. The seasonal and phased light curves. The phased curves are produced by using the main frequency derived from the light curve of that year. The effect of the rotation is seen in each folded light curve.

In the last panel in Figure 7, we display the variation in the frequency at around 2.24 c d^{-1}. As seen in the figure, the variation is correlated with the change seen in the Hα line profile.

7. Discussion

Obtaining more information about the mass loss and disk formation of Be stars is crucial to our understanding of the mechanisms responsible for the Be phenomenon. There are several theories proposed to explain these episodic events. The most discussed assumptions among them are the NRPs and rotational modulations since the majority of Be stars show light and line profile variations. To give some examples, while Walker et al. (2005), Huat et al. (2009), and Neiner et al. (2012) demonstrate the effectiveness of the NRPs, Degroote et al. (2009) and Balona (2016) indicate the role of the rotational modulations in Be stars. The appropriateness of these two hypotheses can be evaluated by comparing the line centres and wings of high-resolution spectra, by examining the light curves and the radial velocities of spectral lines, or by monitoring the photometric variability (Sareyan et al. 1998).

Within this context, we obtain the photometric observations of the star from the *STEREO* satellite between 2007 and 2011, and sensitively investigate the frequency and amplitude variations. We also look at the Hα emission spectra, taken in the same time interval with that of the photometric observations, from the archives and compare the results.

Downloaded from https://www.cambridge.org/core. Ankara Universitesi, on 12 Dec 2021 at 00:02:46, subject to the Cambridge Core terms of use, available at https://www.cambridge.org/core/terms.
https://doi.org/10.1017/pasa.2018.38

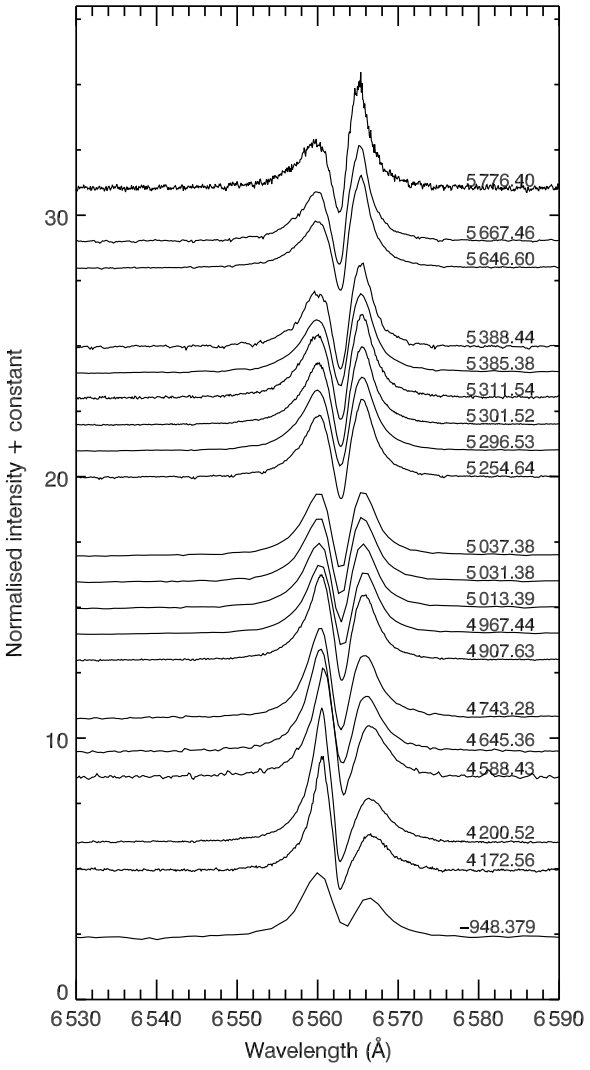


Figure 6. Spectroscopic observations of 48 Lib obtained from the BESS database, taken between 2007 and 2011. The spectra show a strong central absorption line surrounded by violet and red emission components, indicating the existence of a circumstellar disk sector in sight of line. The numbers on the right-hand side are Heliocentric Julian Dates (HJD 2 450 000).

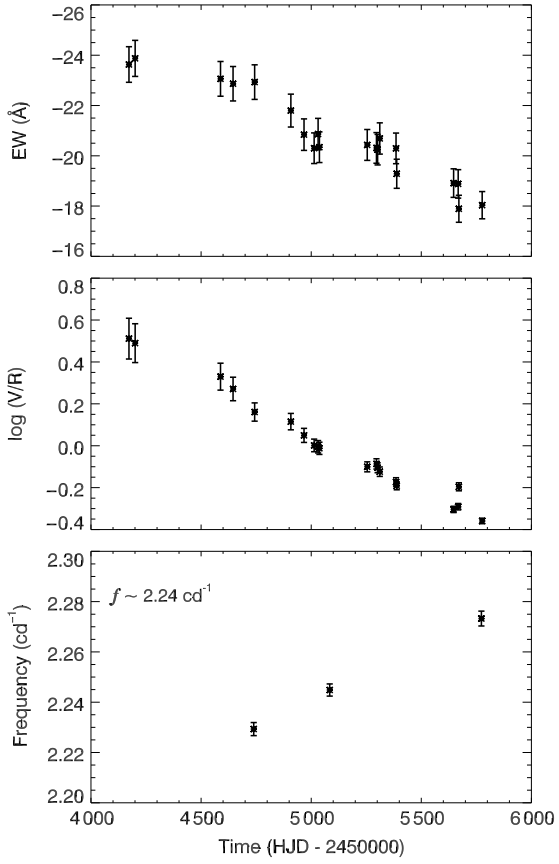


Figure 7. The variations in the EW and V/R ratio of the Hα line as well as in the frequency at around 2.24 c d^{-1}.

In order to estimate the rotational period of the star, we use the period–rotation relation, given as

$$P_{\rm rot} = \frac{50.6 R_\star \sin i}{v \sin i} \,. \qquad (3)$$

For the calculation of $v \sin i$, we derive the critical velocity of the star from $v_{\rm cr} = \sqrt{2GM_\star/3R_{\rm p}}$, where $M_\star$ and $R_{\rm p}$ are the mass and the polar radius of the star and are assumed to be 6.07 $M_\odot$ and 3.12 $R_\odot$, respectively (Silaj et al. 2016). Accordingly, we find the critical velocity to be ∼497 km s^{-1}. Since Silaj et al. (2016) give that $v_{\rm eq}/v_{\rm cr} \approx 0.80$ for 48 Lib, the equatorial velocity ($v_{\rm eq}$) of the star is calculated as ∼398 km s^{-1}. Also, by assuming that the inclination angle is $i = 85°$ (Silaj et al. 2016), the projected rotational velocity ($v \sin i$) is found to be ∼396 km s^{-1}.

From equation (3) and the values determined above, we estimate a rotational period of ∼2.52 c d^{-1}, which is fairly close to the dominant peak at 2.49 c d^{-1} derived from the 5-yr combined light curve. It is also obvious from Figure 2 that the amplitude spectra consist of two dominant frequencies at around 2.49 and 5.00 c d^{-1}, and the variations of these two dominant frequencies are almost identical according to Figure 3. This is a strong evidence that there is really only one periodic variation with its harmonic giving rise to the stable light curve shown in Figures 4 and 5.

This 2:1 frequency formation is best explained by Cameron et al. (2008) with the existence of the dominantly excited prograde modes among the high-order g-modes in Be types. These modes have frequencies of around $|m|\Omega$ in the observer's frame, where $|m|$ is the azimuthal order and Ω is the rotation frequency (Cameron et al. 2008). In a fast rotator, frequencies in the co-rotating frame (f_g) of intermediate- to high-order g-modes are quite smaller than $|m|\Omega$. In this case, the frequencies in the observer's frame are $f_g - m\Omega \approx -m\Omega$, and they produce a group that is close to $\approx |m|\Omega$ or that is separated from other groups by $\approx |m|\Omega$ (Saio 2014). This property makes the photometric period close to the rotation period or half of it (Cameron et al. 2008).

The observational facts, such as the observed dominant period being consistent with the likely rotation period or a single peak and its harmonics on the amplitude spectrum, seen in 48 Lib, are very similar to the typical characteristics of a rotational variable. In this case, the light variations of 48 Lib can be interpreted as a rotational modulation caused by an inhomogeneous region. The inhomogeneity here refers to a co-rotating spot region, whose existence on or just above the photosphere of A- and B-type stars is theoretically and observationally proved by Cantiello & Braithwaite (2011) and Balona (2016), respectively. Also, there are several strong theories suggesting that the periodic variations of Be stars are due to long-lasting co-rotating structures

Downloaded from https://www.cambridge.org/core. Ankara Universitesi, on 12 Dec 2021 at 00:02:46, subject to the Cambridge Core terms of use, available at https://www.cambridge.org/core/terms.
https://doi.org/10.1017/pasa.2018.38

(Balona, Aerts, & Štefl 1999; Balona & Kaye 1999; Balona 2013b). Similar structure above the photosphere of 48 Lib may be responsible for the main periodicity at 2.49 c d^{-1}. Indeed, Hanuschik & Vrancken (1996) discuss the existence of extremely narrow multiple absorption features in Fe II shell lines that are variable in radial velocity and depth on a short timescale for 48 Lib, and they refer this variation to co-orbiting clumps in the disk or a higher-order distortions in the global density wave.

In this study, the coherence of the photometric data with a simple spot model is investigated in order to reveal the presence of such a non-homogeneous structure on or above the photosphere of 48 Lib. As seen in Figure 4, the model constructed by using only one circular spot represents the 5-yr combined light curve fairly well. However, this result is not a definitive solution. The asymmetry in the phased light curve can be better modelled by using more than one spot or by taking differential rotation into account.

The origin of the photometric obscuration is not clear for the star. However, as given by Spruit (2002) and Mullan & MacDonald (2005), there is a possibility that this feature may be a result of a magnetic field produced by the Tayler instability in a differentially rotating star. Also, Cantiello & Braithwaite (2011) suggest that dynamo action in thin subsurface convection zones in hot stars might generate a magnetic field. In this case, magnetic spots can manifest themselves as hot, bright spots. On the other hand, it is not possible to distinguish between bright and dark spots on the basis of the light curves alone. Moreover, Hubrig et al. (2009) state that rapidly rotating Be stars show magnetic fields of the order of less than 100 G. According to Smith (1994), these fields are responsible for the co-rotating structures which arise from mass ejection process through magnetic flaring. In such a process, highly ionised gas is released and trapped in closed magnetic loops. Then, gas escapes along open field lines. It is dragged and accelerated by the rapid rotation of the star. Depending on the rotational velocity, the gas reaches circular orbital speeds at some distance from the star if it is still ionised, and this makes the photometric period close to the rotation period (Balona 2013a).

Handling the relation between the mass loss and disk formation in terms of the rotation, it is known that the star needs to be rotating quite close to its critical rotational velocity to eject material into orbit. However, the equatorial velocity of the star is 398 km s^{-1}, and this value is 80% of its critical value calculated as 497 km s^{-1} (Silaj et al. 2016). Since this percentage is well below the expected value, the rotation alone seems unlikely to be related with mass loss. Therefore, the existence of another mechanism additional to the rotation should be taken into account for 48 Lib. The periodogram of the star contains two low frequencies at 0.109 and 0.199 c d^{-1}, and such frequencies are ascribed to the photometric variability of the long-term outbursts seen in Be stars (Rivinius, Baade, & Carciofi 2016). On the bases of this, it should be considered that bursts with 10-d period in the star may cause above-stated mass-loss event.

Last but not least, Haubois et al. (2012) state that 48 Lib shows a positive correlation between $U-B$ and $B-V$. Although such a behaviour is considered as normal for shell stars (Harmanec 1983), it is determined that the colours are also well associated with long-term V/R variation (McDavid et al. 2000). On this basis, Haubois et al. (2012) suggest that the colour and magnitude changes observed in the star are linked to the azimuthal structure of the disk governed by the one-armed density wave, seen at different aspect angles over the years.

In parallel with this, the results of the photometric and spectroscopic analysis in this study display a correlation in a way that supports the existence of such structure. Accordingly, the decreasing trends of both EW and V/R ratio are inversely proportional to the change in the frequency seen at around 2.24 c d^{-1}. The minimum phase of the quasi-periodic variation observed in the EW values coincides with the maximum levels of the photometric variations seen at 2.20, 2.42, 2.49, and 4.95 c d^{-1} as well as those seen in the amplitudes of 2.20 and 2.59 c d^{-1}. Furthermore, the maximum of the quasi-periodic change in EW on around HJD 2 454 600 (2008 season) shows inverse proportion to the changes at 2.17 and 2.37 c d^{-1}, and to the unusual drop in the main frequencies. Also, it inversely varies relative to the amplitudes of 2.49 c d^{-1} and the main frequencies in the same date, whereas the jumps in the amplitudes of 2.17, 2.32, 2.37, and 2.42 c d^{-1} have a similar variation. Finally, an inverse correlation is observed between the frequencies at 2.42 and 2.59 c d^{-1}, and the maximum of the quasi-periodic structure occurred on HJD 2 455 450 (2010 season).

Although the *STEREO* has a shorter seasonal observation duration and collects less data points compared to other space missions, its high-precision data and uninterrupted monitoring ability enable us to measure photometric variations with great accuracy and provide hints about the relation between the photometric and emission line variations. Also, it gives a chance to gain a better understanding of the origin of the dominant peaks and multi-periodicities seen in the star.

Author ORCIDs. D. Ozuyar, http://orcid.org/0000-0001-8544-0950.

Acknowledgements. We acknowledge assistance from Dr. Vino Sangaralingam, Dr. Gemma Whittaker, Dr. Ibrahim Ozavci, and Zahide Terzioglu in the production of the data used in this study. This work has made use of the BeSS database, operated at LESIA, Observatoire de Meudon, France: http://basebe.obspm.fr. The *STEREO* Heliospheric Imager was developed by a collaboration that included the Rutherford Appleton Laboratory and the University of Birmingham, both in the United Kingdom, and the Centre Spatial de Lige (CSL), Belgium, and the US Naval Research Laboratory (NRL),Washington DC, USA. The *STEREO/SECCHI* project is an international consortium of the Naval Research Laboratory (USA), Lockheed Martin Solar and Astrophysics Lab (USA), NASA Goddard Space Flight Center (USA), Rutherford Appleton Laboratory (UK), University of Birmingham (UK), Max-Planck-Institut fr Sonnen-systemforschung (Germany), Centre Spatial de Lige (Belgium), Institut dOptique Thorique et Applique (France), and Institut dAstrophysique Spatiale (France). This research has made use of the SIMBAD database, opened at CDS, Strasbourg, France. This research has also made use of NASA's Astrophysics Data System.

References

Balona, L. A. 1995, MNRAS, 277, 1547
Balona, L. A. 2009, in AIP Conf. Ser. 1170, ed. J. A. Guzik, & P. A. Bradley, 339, doi:10.1063/1.3246509
Balona, L. A. 2013a, in Astrophy. Space Sci. Proc. 31, Stellar Pulsations: Impact of New Instrumentation and New Insights, ed. J. C. Suárez, R. Garrido, L. A. Balona, & J. Christensen-Dalsgaard, 247, doi:10.1007/978-3-642-29630-7_45
Balona, L. A. 2013b, MNRAS, 431, 2240
Balona, L. A. 2014a, in ed. G. Mathys, E. R. Griffin, O. Kochukhov, R. Monier, & G. M. Wahlgren, Putting A Stars into Context: Evolution, Environment, and Related Stars, 415
Balona, L. A. 2014b, MNRAS, 439, 3453
Balona, L. A. 2016, MNRAS, 457, 3724
Balona, L. A., & Kaye, A. B. 1999, ApJ, 521, 407
Balona, L. A., Aerts, C., & Štefl, S. 1999, MNRAS, 305, 519
Balona, L. A., et al. 2011, MNRAS, 413, 2403
Bewsher, D., Brown, D. S., Eyles, C. J., Kellett, B. J., White, G. J., & Swinyard, B. 2010, SoPh, 264, 433

Downloaded from https://www.cambridge.org/core. Ankara Universitesi, on 12 Dec 2021 at 00:02:46, subject to the Cambridge Core terms of use, available at https://www.cambridge.org/core/terms. https://doi.org/10.1017/pasa.2018.38

Bossi, M., Guerrero, G., Scardia, M., & Tadini, M. 1994, in Be Star Newsletter: Rapid Spectroscopic Variability in the Be Star 48 Lib. 7
Cameron, C., et al. 2008, ApJ, 685, 489
Cantiello, M., & Braithwaite, J. 2011, A&A, 534, A140
Catanzaro, G. 2013, A&A, 550, A79
Collins, II, G. W. 1987, in IAU Colloq. 92, Physics of Be Stars, ed. A. Slettebak, & T. P. Snow, 3
Cranmer, S. R. 2005, ApJ, 634, 585
Cuypers, J., Balona, L. A., & Marang, F. 1989, A&AS, 81, 151
Degroote, P., et al. 2009, A&A, 506, 471
Dorren, J. D. 1987, ApJ, 320, 756
Draper, Z. H., Wisniewski, J. P., Bjorkman, K. S., Meade, M. R., Haubois, X., Mota, B. C., Carciofi, A. C., & Bjorkman, J. E. 2014, ApJ, 786, 120
Eyles, C. J., et al. 2009, SoPh, 254, 387
Floquet, M., Hubert, A. M., Hubert, H., Janot-Pacheco, E., Caillet, S., & Leister, N. V. 1996, A&A, 310, 849
Frémat, Y., Zorec, J., Hubert, A.-M., & Floquet, M. 2005, A&A, 440, 305
Goss, K. J. F., Karoff, C., Chaplin, W. J., Elsworth, Y., & Stevens, I. R. 2011, MNRAS, 411, 162
Gunasekera, S., Adassuriya, J., & Medagangoda, N. I. 2008, SunGe, 3, 67
Gutiérrez-Soto, J., Fabregat, J., Suso, J., Lanzara, M., Garrido, R., Hubert, A.-M., & Floquet, M. 2007, A&A, 476, 927
Gutiérrez-Soto, J., Semaan, T., Garrido, R., Baudin, F., Hubert, A., & Neiner, C. 2010, Preprint (arXiv:1010.1910)
Hanuschik, R. W., & Vrancken, M. 1996, A&A, 312, L17
Harmanec, P. 1983, HvaOB, 7, 55
Haubois, X., Carciofi, A. C., Rivinius, T., Okazaki, A. T., & Bjorkman, J. E. 2012, ApJ, 756, 156
Huat, A.-L., et al. 2009, A&A, 506, 95
Hubrig, S., Schöller, M., Savanov, I., Yudin, R. V., Pogodin, M. A., Štefl, S., Rivinius, T., & Curé, M. 2009, AN, 330, 708
Jones, C. E., Tycner, C., & Smith, A. D. 2011, AJ, 141, 150
Lafrenière, D., Jayawardhana, R., van Kerkwijk, M. H., Brandeker, A., & Janson, M. 2014, ApJ, 785, 47
McDavid, D. 1988, BAAS, 20, 954
McDavid, D., Bjorkman, K. S., Bjorkman, J. E., & Okazaki, A. T. 2000, in ASP Conf. Ser. 214, IAU Colloq. 175: The Be Phenomenon in Early-Type Stars, ed. M. A. Smith, H. F. Henrichs, & J. Fabregat, 460
Mullan, D. J., & MacDonald, J. 2005, MNRAS, 356, 1139
Neiner, C., et al. 2009, A&A, 506, 143
Neiner, C., et al. 2012, A&A, 546, A47
Okazaki, A. T. 1997, A&A, 318, 548
Peña-Guerrero, M. A., & Leitherer, C. 2013, AJ, 146, 158
Percy, J. R. 2007, in Understanding Variable Stars (Cambridge: Cambridge University Press), 350
Porter, J. M., & Rivinius, T. 2003, PASP, 115, 1153
Pott, J.-U., et al. 2010, ApJ, 721, 802
Ramiaramanantsoa, T., et al. 2014, MNRAS, 441, 910
Ringuelet-Kaswalder, A. E. 1963, ApJ, 137, 1310
Rivinius, T., Baade, D., Štefl, S., Stahl, O., Wolf, B., & Kaufer, A. 1998, A&A, 336, 177
Rivinius, T., Baade, D., & Štefl, S., 2003, A&A, 411, 229
Rivinius, T., Carciofi, A. C., & Martayan, C. 2013, A&A Rev., 21, 69
Rivinius, T., Baade, D., & Carciofi, A. 2016, Preprint (arXiv:1608.02872)
Saio, H. 2014, (arXiv:1309.7249)
Saio, H., et al. 2007, ApJ, 654, 544
Sangaralingam, V., & Stevens, I. R. 2011, MNRAS, 418, 1325
Sareyan, J. P., et al. 1998, A&A, 332, 155
Silaj, J., et al. 2016, ApJ, 826, 81
Smith, M. A. 1994, in IAU Symp. 162, Pulsation; Rotation; and Mass Loss in Early-Type Stars, ed. L. A. Balona, H. F. Henrichs, & J. M. Le Contel, 241
Spruit, H. C. 2002, A&A, 381, 923
Touhami, Y., et al. 2013, ApJ, 768, 128
Townsend, R. H. D., Owocki, S. P., & Howarth, I. D. 2004, MNRAS, 350, 189
Walker, G. A. H., et al. 2005, ApJ, 635, L77
Whittaker, G. N., Stevens, I. R., & Sangaralingam, V. 2013, MNRAS, 431, 3456
Zorec, J., & Briot, D. 1997, A&A, 318, 443
Štefl, S., Le Bouquin, J.-B., Carciofi, A. C., Rivinius, T., Baade, D., & Rantakyrö, F. 2012, A&A, 540, A76

Downloaded from https://www.cambridge.org/core. Ankara Universitesi, on 12 Dec 2021 at 00:02:46, subject to the Cambridge Core terms of use, available at https://www.cambridge.org/core/terms.
https://doi.org/10.1017/pasa.2018.38